Available online at www.sciencedirect.com
SCIENCE DIRECT®
Journal of Solid State Chemistry 177 (2004) 2896–2902
JOURNAL OF SOLID STATE CHEMISTRY
http://elsevier.com/locate/jssc

Phase transition induced by lithium insertion in α_I- and α_{II}-$VOPO_4$

N. Dupré,[a] G. Wallez,[a,*] J. Gaubicher,[b] and M. Quarton[a]

[a] *Laboratoire de Cristallochimie du Solide, Institut des Matériaux de Paris-Centre, Université Pierre et Marie Curie-Paris VI, 4 place Jussieu, Tour 54-44, 75252 Paris Cedex 05, France*

[b] *Institut des Matériaux Jean Rouxel, 2, rue de la Houssinière, BP 32229, 44322 Nantes Cedex 3, France*

Received 2 December 2003; received in revised form 1 April 2004; accepted 2 April 2004

Abstract

Lithium insertion in α_I-$VOPO_4$ and α_{II}-$VOPO_4$, either by chemical or electrochemical route, leads to the same new compound: α_I-$LiVOPO_4$ (space group $P4/nmm$). The structure, resolved by neutron and synchrotron diffraction, is made up of planes of corner-connected PO_4 and VO_5 polyhedra, whereas lithium atoms are located between the layers. The reversal of the short vanadyl bond that corresponds to the insertion-induced α_{II}–α_I transition finds an explanation in terms of lattice energy. It favors the migration of lithium ions in the (0 0 1) interlayer planes, a key parameter for the electrochemical performance as electrode material in Li-ion batteries.

Keywords: Crystal structure; Lithium battery material; Electrochemical intercalation; Phosphate; Neutron diffraction; Synchrotron diffraction

1. Introduction

The present work is part of a research program dealing with new cathode materials for lithium intercalation. So far, numerous investigations in this field have been dedicated to simple oxides, but recent works have shown up that the $VOXO_4$ compounds (X = P, S) also showed attractive performance, with operating potential near 4 V, specific capacity exceeding 100 mA h g^{-1} and good cyclability [1,2]. Beside the electrochemical experiments that aim to improve these materials, we have undertaken a structural study on the lithiated forms of $VOPO_4$ in order to clear up the intercalation mechanisms.

Depending on the synthesis conditions, $VOPO_4$ crystallizes under numerous forms, but all those known to this date are made up of VO_6 octahedra sharing vertices with independent PO_4 tetrahedra. The oxygen polyhedron of vanadium is so irregular that it is often considered as a VO_5 square pyramid with a very short apical vanadyl bond ($d_{V=O}$ = 1.58 Å in the α_{II} form) and a much more remote sixth oxygen atom ($d_{V\cdots O}$ = 2.85 Å). The $VOPO_4$ forms mainly differ by the orientation of the vanadyl bond, however, they all generate infinite O=V···O=V··· chains. The heretonow known structural forms are (Fig. 1):

- α_I-$VOPO_4$ obtained by dehydration of α-$VOPO_4 \cdot 2H_2O$ at 250°C has not yet been fully characterized, but it is assumed to be isotypic with α-$VOSO_4$ [3], that is, lamellar, with alternating *antiparallel* V=O bonds pointing *inside* the layers, the interplanar cohesion being due to the V···O bonds;
- α_{II}-$VOPO_4$ forms after 1 h at 695°C; the V=O bonds are also *antiparallel*, but contrary to those of α_I-$VOPO_4$, they point *outside* the layers and partly clutter up the interplanar space [4];
- γ-$VOPO_4$ forms after 3 days at the same temperature as α_{II}; it is supposed to be an intermediate form between those of α_I and α_{II}, with all V=O bonds *parallel* and pointing *half inside*, *half outside* the layers [5];
- δ-$VOPO_4$ obtained by dehydration of $VOHPO_4 \cdot 1/2H_2O$ followed by 1 week heat treatment at 450°C, is supposed to have a slightly more complex

*Corresponding author. Fax: +33-1-44-27-25-48.
E-mail address: gw@ccr.jussieu.fr (G. Wallez).

0022-4596/$ - see front matter © 2004 Elsevier Inc. All rights reserved.
doi:10.1016/j.jssc.2004.04.006

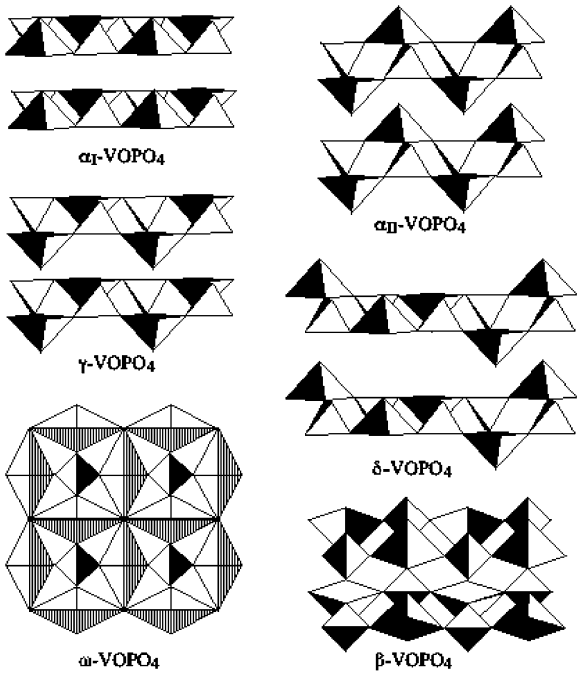

Fig. 1. Schematic view of the different forms of $VOPO_4$. Square pyramids are VO_5 (disordered "double pyramids" for the ω-form) and tetrahedra are PO_4.

structure, with *antiparallel* V=O bonds pointing *half inside*, *half outside* the layers [6];

- ω-$VOPO_4$ obtained by slow heating of $VOHPO_4 \cdot nH_2O$ ($n=2$, 4) in air, shows disordered vanadyl chains in the [1 0 0] and [0 1 0] directions of the tetragonal cell [7];
- in β-$VOPO_4$, the only form observed above and after cooling from 700°C, the V=O bonds are tilted so as to form zig-zag O=V···O=V··· chains [8], contrary to all the other $VOPO_4$ forms, successive layers are connected via PO_4 tetrahedra;
- ε-$VOPO_4$, obtained under hydrothermal conditions, is supposed to be related to the β-form [9].

It should be noted that except for the β form, the slight differences between the synthesis conditions often lead to mixtures, notably for α_{II}-, γ-, and δ-$VOPO_4$. For that reason, as well as the low crystallinity of most of these phases, the structural characterization of $VOPO_4$ is still uncompleted. Moreover, the knowledge of its lithiated forms appears even more deficient, with only two forms that are known: monoclinic obtained from the melt by Lavrov et al. [10] and orthorhombic prepared hydrothermally by Lii et al. [11], both belonging to the β-type. Furthermore, no electrochemically lithiated form of $VOPO_4$ has ever been structurally characterized.

We recently observed that oxidation and dehydration of $VOHPO_4 \cdot 1/2H_2O$ (680°C, 12 h, under O_2 flow) yielded to micron-sized α_{II}-$VOPO_4$ with thin superficial impurities of the γ form [2]. This so-called "α_{II}-$VOPO_4$-*p*" material shows a lower tendency to aggregate than the pure phase and therefore, a better specific capacity for lithium intercalation (80 vs. 12°mA h g^{-1} upon 40 cycles at a C/5 regime). The potential hysteresis on the voltamograms showed that the lithium electrochemical insertion in this compound was indeed a two-phase phenomenon [2]. These previous results, as well as the interesting performance of α_{II}-$VOPO_4$ as a host material for lithium ions, led us to carry out a structural study of the fully lithiated form.

2. Experimental procedures

2.1. Samples preparations

α_I-$VOPO_4$ that was used as the starting material for lithiation, has been synthesized as previously described [3]. α_{II}-$VOPO_4$ has been obtained by dehydration of $VOPO_4 \cdot 2H_2O$ (1 h, 695°C, under air) (2), but the sample contains 24% β-$VOPO_4$ (inferred from Rietveld refinement). Indeed, it is very difficult to obtain a lower β-$VOPO_4$ content because of the extreme closeness of the synthesis temperatures.

For electrochemical insertion, the products were mixed with acetylene black carbon and PVDF as the binder (75, 20, and 5 wt%, respectively). The slurries were casted from a suspension of this mixture in cyclopentanone on aluminum disks and dried under vacuum. Swagelock™-type cells were used for electrochemical experiments with lithium metal as the negative and reference electrode and 1 M $LiClO_4$ solution in ethylene carbonate/dimethylene carbonate as the electrolyte. The electrochemical reduction was performed in galvanostatic mode by McPile system [12] from 4.0 to 3.0 V at a C/50 regime until nearly one electron per formula unit was inserted. Along with minor impurities due to the additives, the powder pattern showed the presence of orthorhombic β-$LiVOPO_4$ [11] and the supposingly fully intercalated forms of α_I- and α_{II}-$VOPO_4$.

Regarding the chemical lithiation, the sample was mixed with a five-fold excess of LiI in acetonitrile, sealed under argon and stirred up for 2 weeks at room temperature, then filtered, washed with acetonitrile and dried under vacuum. Element analysis for the inserted α_I-$VOPO_4$ sample gives a Li/V = 0.96(2) molar ratio, that accounts for a nearly complete reaction. In the following, we will consider that the sample obeys to the $LiVOPO_4$ formula.

2.2. Diffraction and structure determination

A preliminary XRD study of the four so-obtained samples showed very strong similarities between them.

They are all tetragonal, with close cell parameters: $a = 6.28 \pm 0.01$ Å and $c = 4.444 \pm 0.003$ Å. Further diffraction experiments were undertaken in order to demonstrate this analogy, the first one on an electrochemically lithiated α_{II}-$VOPO_4$ sample (EC), the second one on a chemically lithiated α_I-$VOPO_4$ sample (C).

The internal volume of the electrochemical cell allows to prepare only small amounts of the EC-lithiated material. Therefore, the most convenient way to study its crystal structure was to use the synchrotron radiation. A glass capillary was filled under dried argon with the inserted material, then sealed. The powder data were collected at ESRF (Grenoble, France), then combined into 0.005° bins for structural analysis. The C-lithiated material can be easily prepared in sufficient large amounts to fill up a $3\,cm^3$ vanadium container for neutron diffraction, carried out at the Institut Laüe-Langevin (Grenoble, France). Operating conditions are reported in Table 1.

The Rietveld refinements (Fig. 2) for both samples were performed with *Fullprof.2k* [13], using the cell parameters and atomic positions of α_{II}-$VOPO_4$ [4] as starting data set. β-$LiVOPO_4$ [11] was taken into account in the treatment of the pattern of the EC sample. The cell volume difference ($V_{EC} - V_C = 0.75(3)$ Å^3) is faint and may result from slight differences in the lithiation rates. It is clearly lower than between initial α_{II}-$VOPO_4$ and EC-α_I-$LiVOPO_4$ (8 Å^3).

Because the cell parameters ratio $a/c = 1.415$ is very close to $\sqrt{2}$, the diffraction peaks with equal $(h^2 + k^2 + 2 \times l^2)$ have the same d_{hkl}, like 1 1 1 and 2 0 0; 0 0 2 and 2 2 0; 1 1 2, 2 2 1 and 3 1 0 and so on. A considerable deal of information is lost because of peak overlaps, therefore, we preferred to use isotropic temperature factors for all atoms in order to reduce the number of intensity-dependent variables. The

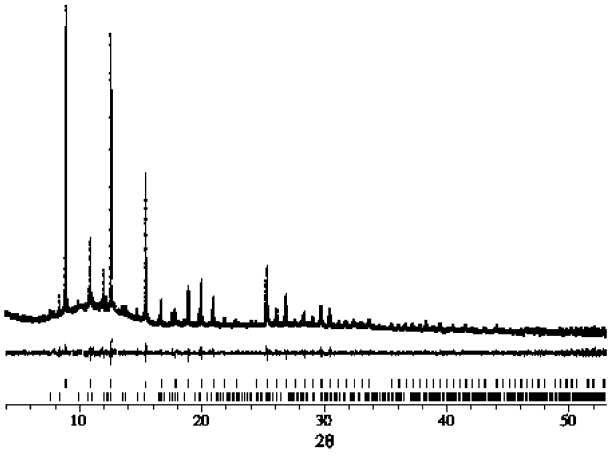

Fig. 2. Synchrotron Rietveld plot: observed (dots), calculated (solid) and angular positions of possible Bragg reflections for α_I-$LiVOPO_4$ (upper bars) and β-$LiVOPO_4$ (lower bars), lower plot: ($I_c - I_o$) difference curve.

Table 1
Data collection, refinement conditions and crystallographic data

	EC-α_I-$LiVOPO_4$	C-α_I-$LiVOPO_4$
Data collection		
Powder holder	Glass capillary	Vanadium container
Temperature	293 K	293 K
Apparatus	ESRF-BM16 beamline	ILL-D2B beamline
Radiation, λ, monochromator	synchrotron, 0.68891 Å, Ge (1 1 1)	neutron, 1.5938 Å, Ge (1 1 1)
Scan limits, step	$4.00 < 2\theta < 53.50°$, 0.005°	$14.00 < 2\theta < 159.50°$, 0.05°
Observed reflections	147	123
Refinement conditions		
I-dependent parameters	9 (x, z and B_{iso} fixed for Li)	11 (B_{iso} fixed for V)
Profile parameters	10	10
Conventional reliability factors[a]	$R_P = 0.046$	$R_P = 0.018$
	$R_{WP} = 0.049$	$R_{WP} = 0.023$
	$R_{Bragg} = 0.034$	$R_{Bragg} = 0.031$
	$R_{exp} = 0.047$	$R_{exp} = 0.013$
	$R_F = 0.032$	$R_F = 0.022$
	$\chi^2 = 1.07$	$\chi^2 = 3.09$
Crystallographic data		
System, space group	Tetragonal, $P4/nmm$ (n · 129)	
Cell parameters, volume	$a = 6.2910(1)$ Å	$a = 6.2797(2)$ Å
	$c = 4.4452(1)$ Å	$c = 4.4423(4)$ Å
	$V = 175.92(1)$ Å^3	$V = 175.18(2)$ Å^3
Formula weight, Z, calc. density	167.81 g mol^{-1}, 2, 3.17 g cm^{-3}	

[a] $R_P = \Sigma|y_o^i - y_c^i|/\Sigma y_o^i$, R_{WP} (id., weighted); $R_{Bragg} = \Sigma|I_o^i - I_c^i|/\Sigma I_o^i$; $R_{exp}((n-p)/\Sigma w_i y_o^i)^{1/2}$; $R_F = \Sigma|(I_o^i)^{1/2} - (I_c^i)^{1/2}|/\Sigma(I_o^i)^{1/2}$; $\chi^2 = (R_{WP}/R_{exp})^2$.

localization of the lithium cations led us to consider various structural schemes that will be discussed below. The conditions for the final refinements are reported in Table 1.

3. Results and discussion

In α_{II}-$VOPO_4$ (space group $P4/nmm$) [4], the O(2) atom splits into two symmetrical positions at $x = 0.196(1)$ and $0.304(1)$, on both sides of a m mirror at $x = 1/4$, resulting in a slight folding of the oxygen network and a shrinkage in the $(\boldsymbol{a}, \boldsymbol{b})$ plane. In the lithiated form, attempts have been made to refine the O(2) atom on the same way, but the obtained position ($x = 0.251(2)$ for EC form; $x = 0.250(4)$ for the C one) was so close to the mirror plane that it has been eventually considered as located at $x = 1/4$ (Fig. 3). This difference between α_{II}-$VOPO_4$ and its intercalated form may simply result from an "inflating" steric effect of the lithium cations that gives the oxygen network its maximum volume (+5%) and prevents the possible oscillations between the symmetrical forms.

The most outstanding structural modification caused by the intercalation is the atomic displacement following **c**: synchrotron diffraction shows that the V atom shifts from $z = 0.2139(5)$ [4] to 0.4186(4) (+0.90 Å, taking the barycenter of the layer (n-plane at $z = 1/2$) as reference) while the apical O(1) atom shifts inversely from $z = 0.858(2)$ to 0.775(1) (−0.37 Å). A similar position is observed for O(1) by neutron diffraction in the C sample, but the very faint Fermi length of the vanadium atom does not allow to locate it as accurately as by synchrotron diffraction. The result of these shifts after lithium insertion in α_{II}-$VOPO_4$ is a reversal of the V═O(1) vanadyl bond that turns from outside toward inside the layer (Fig. 4), leading to an α_I-like oxygen framework, that is, a perfect 2D structure. So, the electrochemical and chemical reactions can be summarized as follows:

$$\text{(EC)}\quad \alpha_{II}\text{-}V^{V}OPO_4 + Li \rightarrow \alpha_I\text{-}LiV^{IV}OPO_4,$$

$$\text{(C)}\quad \alpha_I\text{-}V^{V}OPO_4 + Li \rightarrow \alpha_I\text{-}LiV^{IV}OPO_4.$$

Compared to that of α_{II}-$V^{V}OPO_4$, the sum of the V═O(1) and V⋯O(1) bond lengths (parameter c) does not increase significantly with insertion (+0.2%), but the four "equatorial" V-O(2) bonds stretch by nearly 0.1 Å as a result of the reduction of the V^{V} cation to V^{IV}.

Due to its low weight, the lithium atom cannot be observed precisely by X-ray diffraction in the neighborhood of heavier atoms like vanadium. Therefore, we will mostly relied on neutron diffraction for its localization. An examination of the α_I framework reveals two vacant C_{2h} octahedral sites in which the lithium may insert, one inside the polyhedra layer (l, 4e site), the other one in the interlayers space (i, 4d site). Firstly, we made various refinement attempts on the neutron pattern in order to determine the occupancy rate (τ) of each site, with lithium atoms supposed to lie at the centers of the octahedra. These results are consistent with a nearly complete insertion:

- with bound occupancy rates ($\tau_l + \tau_i = 1$, that is, 1 lithium per formula): $\tau_l = 0.00(2)$, $\tau_i = 1.00(2)$;
- with free occupancy rates: $\tau_l = 0.03(3)$, $\tau_i = 1.05(3)$.

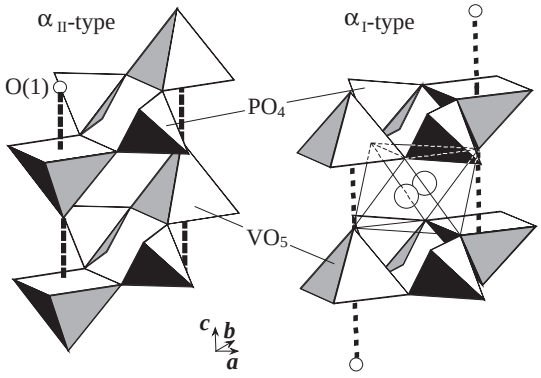

Fig. 4. O═V⋯O inversion by lithium insertion: the α_{II}–α_I transition.

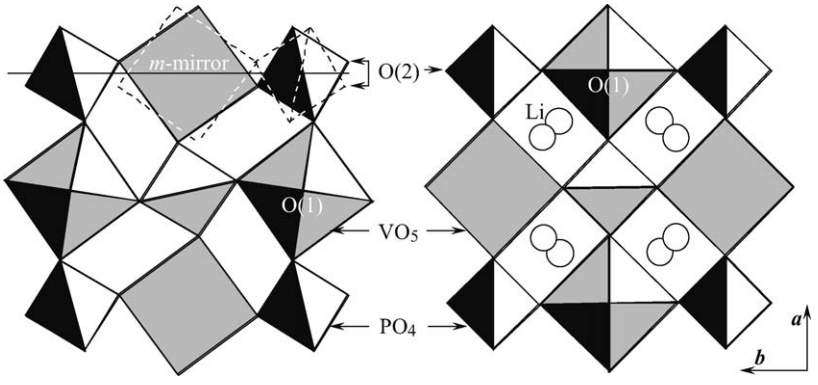

Fig. 3. [0 0 1] projection of α_{II}-$VOPO_4$ (left) and its lithiated form (right).

This clear preference is not surprising considering that the interlayers site is 2.42 Å distant from the two apical O(1) atoms and 2.06 Å from the four O(2), vs., respectively, 2.55 and 1.85 Å for the site inside the layers. Therefore, the former appears more hospitable for a lithium cation ($r(Li^+) = 0.76$ Å) [14] in a six-fold coordination) than the latter. Furthermore, the tilt of the O(1)–O(1) axis with the "equatorial" rectangle formed by the O(2) atoms is more favorable (closer to 90°) in the *i*-octahedron than in the *l*-one: 82° vs. 71°. So, in the following, we will consider the interlayers octahedron as the only one suitable for lithium. The environment of the octahedron center is still irregular however, and suggests that the lithium cation would rather occupy an off-centered 8*j* position on the *m*-mirror plane. Refinements without constraints led to split the lithium site into two symmetrical positions 0.53 Å apart with five-fold coordination, closer to the O(1) vertices. The R_{Bragg} factor is not significantly better than for the previous model (0.031 instead 0.032), but the bond lengths are more regular and more realistic. The lithium cation was blocked on this position for the final refinement of the synchrotron pattern.

So, one may consider that after complete intercalation, the lithium cations occupy half of the interlayers octahedra, that is, 25% of the 8*j* sites. Insofar as a careful observation of the background of the powder patterns does not reveal any superstructure peak, we assume that these cations insert randomly in the octahedra. A comparison between the synchrotron patterns of initial α_{II}-$VOPO_4$ and its electrochemically lithiated form allowed to observe an isotropic broadening of the peaks, regardless of their Miller indexes. Insofar as the size and shape of the grains is not supposed to change during the insertion process, this broadening probably results from an inhomogeneous distribution of the lithium cations. Final atomic positions are given in Table 2 and cations–anions distances in Table 3.

Even under soft chemistry conditions, the lithium insertion can cause reversible structural transitions in polyanions frameworks. In $V_2(SO_4)_3$, for example, two VO_6 octahedra corner-connected by three SO_4 tetrahedra become directly edge-connected after lithiation, releasing tetrahedra corners that bond to the lithium [17]. Beside the valence change of the transition element, this results also from the polarizing power of the small lithium cation. In the case of α_{II}-$VOPO_4$, the transition is only displacive insofar as the reduced vanadium cation simply moves through the square base of its pyramid. This observation is fully consistent with the previous electrochemical study [2], that accounted for a reversible two-phase phenomenon. Furthermore, the simple fact that the four synthesis routes explored lead to the same α_I-type structure, rather than a α_{II}-one, account for a higher stability of the former when lithium is inserted. A comparison of the Coulombic interactions in the so-formed α_I-$LiVOPO_4$ and an hypothetical α_{II}-$LiVOPO_4$ form could explain this structural preference. For this purpose, a model for α_{II}-$LiVOPO_4$ was built, with the same cell parameters and all V–O and P–O

Table 3
Selected interatomic distances (Å) and cumulated bond strengths (v.u., italics) [16] in LiO_6, VO_6 and PO_4 polyhedra for EC-α_I-$LiVOPO_4$ and C-α_I-$LiVOPO_4$

	EC-α_I-$LiVOPO_4$/ synchrotron	C-α_I-$LiVOPO_4$/ neutron
Li–O(1)	2.18	2.16(2)
Li–O(1)	2.70	2.68(2)
Li–O(2) (2 ×)	2.10	2.08(2)
Li–O(2) (2 ×)	2.11	2.08(2)
	0.9	*0.9*
V–O(1)	1.583(5)	1.63(6)
V–O(1)	2.862(5)	2.81(6)
V–O(2) (4 ×)	1.950(2)	1.97(2)
	4.3	*4.0*
P–O(4) (× 4)	1.543(2)	1.554(1)
	4.8	*4.6*

Table 2
Fractional atomic coordinates (cell origin on inversion center) [15] and thermal parameters (Å^2) for EC-α_I-$LiVOPO_4$ and C-α_I-$LiVOPO_4$ (italics)

Atom	*x*	*y*	*z*	B_{iso}	Site	Occupancy
Li	−0.024[a]	1/2−*x*	0.034[a]	0.9[a]	8*j*	1/4
	−0.024(2)		*0.034(6)*	*0.9(3)*		
V	1/4	$\frac{1}{4}$	0.4181(4)	1.33(5)	2*c*	1
			0.42(1)	*1 (fixed)*		
P	1/4	$\frac{3}{4}$	1/2	0.82(6)	2*b*	1
				0.78(4)		
O(1)	1/4	$\frac{1}{4}$	0.774(1)	0.5(1)	2*c*	1
			0.7835(8)	*1.70 (6)*		
O(2)	1/4	0.9512(4)	0.3014(4)	0.68(6)	8*i*	1
		0.9491 (2)	*0.2923 (3)*	*1.26 (2)*		

[a] Fixed as determined by neutron.

distances equal to those of α_I-$LiVOPO_4$ ($z(V) = 0.1814$; $z(O(1)) = 0.8247$; all other atomic coordinates unchanged). Contrarily with α_I-$LiVOPO_4$, the octahedral cavities located inside the layers formed by the PO_4 and VO_5 polyhedra appear as the only ones suitable for hosting lithium ions in a α_{II}-type structure. Actually, those between the layers are clearly inhospitable, as shown by the distances to the centers of the octahedra (C):

- d(C–O(1)) = 2.09 Å (2 ×) and d(C–O(2)) = 2.34 Å (4 ×) (inside layers),
- d(C–O(1)) = 1.82 Å (2 ×) and d(C–O(2)) = 2.67 Å (4 ×) (between layers).

To allow a direct comparison, it will be convenient in the following to set the Li atoms of both models at the center of their oxygen polyhedra. The Li–O(1) mean distance in the α_I-$LiVOPO_4$ model is slightly shorter (2.34 Å) than in α_{II}-$LiVOPO_4$ (2.52 Å), but the Li–O(2) distance remains unchanged.

As shown in Fig. 5, significant differences between the two models appear among the *second* neighbors of the lithium cations, because the LiO_6 octahedron shares faces with two VO_5 pyramids in the layers of the α_{II}-model and Li^+ gets closer to the vanadium cations (twice 2.42 Å instead of twice 2.90 and 3.41 Å). Calculation of the corresponding lattice energies was performed to support this observation, using Ewald's method [18] formulated by Tosi [19]. Consistently with the low ionicity of the compound, various models of partial electric charges were considered (in electronic units, for $LiV^{IV}OPO_4$):

- model A is based upon the ionicity of bonds calculated by Guo et al. [20]: $q_{Li} = 0.78$, $q_V = 3.08$, $q_P = 1.98$, $q_O = -1.168$;
- model B is based upon the electronegativities of Pauling [21]: $q_{Li} = 0.63$, $q_V = 1.90$, $q_P = 1.50$, $q_O = -0.806$.

For both models, oxygen anions received a balancing negative charge. Convergence was reached by integrating potentials generated by a $5 \times 5 \times 7$ crystal cell volume on the various occupied sites of the central cell.

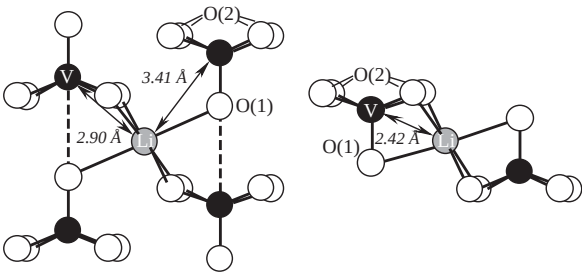

Fig. 5. Comparison of the Li–V interactions between the actual α_I-$LiVOPO_4$ form (left) and the hypothetical α_{II}-$LiVOPO_4$ form (right).

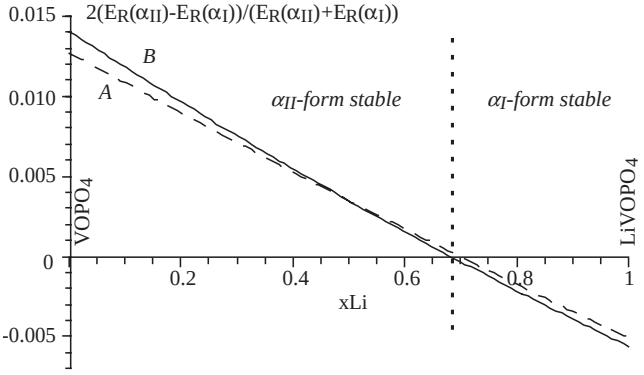

Fig. 6. Lattice energy relative difference between actual α_I-$LiVOPO_4$ form and the hypothetical α_{II}-$LiVOPO_4$ form (E_R's are positive definite). A and B refer to the ions charge models.

Calculations were also performed with simulated oxidation states of vanadium and corresponding intercalation rates of the lithium, i.e. formulae $Li_xV^V_{1-x}V^{IV}_xOPO_4$ $Li_xV^V_{1-x}V^{IV}_xOPO_4$ with $0 \leqslant x \leqslant 1$. Although the model may appear somewhat rough, the stability criterion is the *difference* between the calculated lattice energies of the two forms, not the energies themselves, therefore, the errors in modeling the first-neighbor interactions (equal in the two models, except between Li and O(1)) cancel out. Fig. 6 shows the relative difference between the lattice energies (positive definite) of the two forms vs. Li intercalation rate. According to both models, it appears that the α_I-form is more stable than that of the α_{II} for high insertion rates, but the energy difference is low and the frontier near $x(Li) = 0.7$ is to be considered with cautiousness.

Phase transitions induced by lithium insertion have already been observed in other $VOPO_4$ forms. For example, both chemical and electrochemical lithiations of ε-$VOPO_4$ [22] lead to the monoclinic $LiVOPO_4$ obtained from the melt by Lavrov et al. [10]. Although little is known about the structure of the former, the differences in the powder patterns are evidences of a structural change. Up to this date, the only complete structural study of a lithium insertion in a vanadyl phosphate dealt with the β-form. Its structural transformation upon lithium insertion is slighter than for α_{II}-$VOPO_4$ [8,11,23], but can be explained in similar structural terms: in β-$LiVOPO_4$, the Li^+ cation are located in an almost regular oxygen octahedron ($2.03 \leqslant Li–O \leqslant 2.19$ Å) sharing only edges (no face) with the neighbor VO_5 pyramids, so the shortest Li–V distances are 2.86 Å, close to those of α_I-$LiVOPO_4$ (2.77 Å). One can also note that the volume increase per formula unit is much more important between α_{II}-$VOPO_4$ and α_I-$LiVOPO_4$ (80–88 Å^3; +10%) than between β-$VOPO_4$ and β-$LiVOPO_4$ (83–84 Å^3; +1%): for sterical reasons, a deep structural transformation is necessary in the first case, not in the second one.

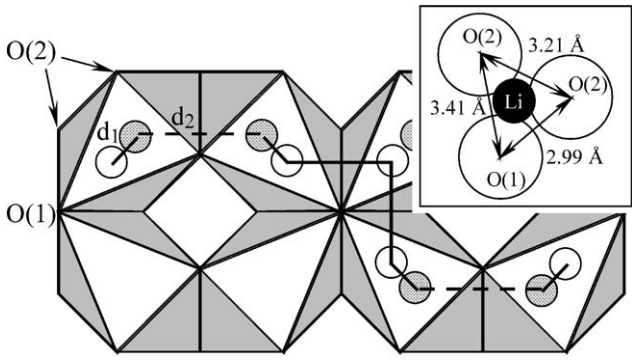

Fig. 7. Lithium migration ways in the (0 0 1) plane of α_I-$LiVOPO_4$. Hatched lithium atoms are below medium plane; dashed lines represent inter-octahedra jumps trough hidden faces. Note that only 1/4 of the sites are occupied in α_I-$LiVOPO_4$. Right upper corner: a LiO_6 octahedron face, with ions at relative size.

Insofar as the mobility of the lithium cations in the host structure is a key parameter for the electrochemical performance, an examination of the migration paths in the present compound has been undertaken. As shown in Fig. 7, the 2D structure of the α_I-form offers a dense network of edge-connected LiO_6 octahedra in the (0 0 1) plane. Migration arises from cation jumps:

- between the two sites of the same octahedron ($d_1 = 0.53$ Å);
- between sites of two adjacent octahedra ($d_2 = 2.83$ Å).

During the latter, the lithium cation must cross two edge-connected O(1)–O(2)–O(2) octahedra faces; this is made possible by the non-compactness of the oxygen packing (Fig. 7).

Ionic conductivity following the ***c***-axis seems improbable, insofar as it would require cation jumps between 4.44 Å distant consecutive interlayer spaces. Such a migration could only occur via the octahedral sites of the layers, which, as shown before, are too narrow for a lithium cation. So, ionic conductivity in α_I-$LiVOPO_4$ can be seen as a 2D phenomenon. The low occupancy rate of the lithium sites (1/4 for α_I-$LiVOPO_4$) is also a favorable criterion for this lithium mobility.

4. Conclusion

Because of its higher stability, α_I-$LiVOPO_4$ appears logically as the product of the chemical and electrochemical lithiations of both α_I- and α_{II}-$VOPO_4$ forms. It is indeed the first known $LiVOPO_4$ form with a 2D structure that lends itself to lithium insertion. The study of the further structural transformations of these host materials during electrochemical cycling is in progress. The rich—and still widely unknown—polymorphism of this promising electrode material may allow other transformations that deserve a full structural investigation of both inserted as non-inserted forms. From a better knowledge of the underlying mechanisms, improvements of the capacity, potential and cyclability may still be expected by chemical substitutions or appropriate synthesis conditions. Further crystallographic works dedicated to the other forms are in progress, along with electrochemical studies.

Acknowledgments

The authors thank Drs. Michella Brunelli of ESRF, Emmanuelle Suard and Jean-Louis Soubeyroux of ILL for their precious help in the diffraction experiments.

References

[1] N. Dupré, J. Gaubicher, T. Le Mercier, G. Wallez, J. Angenault, M. Quarton, Solid State Ionics 140 (2001) 209.
[2] N. Dupré, J. Gaubicher, J. Angenault, G. Wallez, M. Quarton, J. Power Sources 97–98 (2001) 532.
[3] H.A. Eick, L. Kihlborg, Acta Chem. Scand. 28 (1996) 722.
[4] B. Jordan, C. Calvo, Can. J. Chem. 51 (1973) 2621.
[5] E. Bordes, Catal. Today 1 (1987) 499.
[6] F. Benabdelouabad, J.C. Volta, R. Olier, J. Catal. 148 (1994) 334.
[7] P. Amoros, M.D. Marcos, M. Roca, J. Alamo, A. Beltran-Porter, D. Beltran-Porter, J. Phys. Chem. Solids 62 (2001) 1393.
[8] R. Gopal, C. Calvo, J. Solid State Chem. 5 (1972) 432.
[9] S.C. Lim, J.T. Vaughey, W.T.A. Harrison, L.L. Dussack, A.J. Jacobson, J.W. Johnson, Solid State Ionics 84 (1996) 219.
[10] A.V. Lavrov, V.P. Nikolaev, G.G. Sadikov, M.A. Porai-Koshits, Sov. Phys. Dokl. Engl. Transl. 27 (1982) 680.
[11] K.H. Lii, C.H. Li, C.Y. Cheng, S.L. Wang, J. Solid State Chem. 95 (1991) 352.
[12] C. Mouget, Y. Chabre, Multichannel Potentiostat Galvanostat "Mac Pile", licenced from CNRS and UJF-Grenoble to Bio-Logic, 1 Av. de l'Europe, F-38640 Claix, France.
[13] J. Rodriguez-Carvajal, FullProf.2k: Rietveld, Profile Matching and Integrated Intensity Refinement of X-ray and Neutron Data, V 1.9c, Laboratoire Léon Brillouin, CEA, Saclay, France, 2001.
[14] R.D. Shannon, Acta Crystallogr. A 32 (1976) 751.
[15] International Tables for X-ray Crystallography, Vol. A, D. Reidel Publishing Company, Dordrecht, 1987.
[16] N.E. Brese, M. O'Keeffe, Acta Crystallogr. B 47 (1991) 192.
[17] G.B.M. Vaughan, J. Gaubicher, T. Le Mercier, J. Angenault, M. Quarton, Y. Chabre, J. Mater. Chem. 9 (1999) 2809.
[18] P.P. Ewald, Ann. Phys. 64 (1921) 253.
[19] M.P. Tosi, Solid State Phys. 16 (1964) 1.
[20] Y.Y. Guo, C.K. Kuo, P. Nicholson, Solid State Ionics 123 (1999) 225.
[21] L. Pauling, The Nature of the Chemical Bond, Cornell University Press, New York, 1939.
[22] T.A. Kerr, J. Gaubicher, L.F. Nazar, Electrochem. Solid State Lett. 3 (10) (2000) 460.
[23] J. Gaubicher, T. Le Mercier, Y. Chabre, J. Angenault, M. Quarton, J. Electrochem. Soc. 146 (1999) 4375.